

# Direct Observation of Picosecond Lattice Deformation of $\text{Ge}_2\text{Sb}_2\text{Te}_5$ by X-ray Free-Electron Laser

Kazuya Tokuda<sup>1</sup>, Tomoya Kawaguchi<sup>1</sup>, Masashi Sakaida<sup>1</sup>, Takahiro Sato<sup>2,a</sup>, Tadashi Togashi<sup>3</sup>, Kanade Ogawa<sup>2</sup>, Makina Yabashi<sup>2</sup>, Tetsu Ichitsubo<sup>1</sup>, Toshiyuki Matsunaga<sup>4</sup>, Yoshihito Tanaka<sup>2</sup>, Yoshinori Nishino<sup>5</sup>, Noboru Yamada<sup>1</sup>, and Eiichiro Matsubara<sup>1</sup>

<sup>1</sup>Department of Materials Science and Engineering, Kyoto University, Kyoto 606-8501, Japan

<sup>2</sup>RIKEN SPring-8 Center, RIKEN, Hyogo 679-5148, Japan

<sup>3</sup>Japan Synchrotron Radiation Research Institute, Hyogo 679-5198, Japan

<sup>4</sup>Device Solutions Center, Panasonic, Osaka 570-8501, Japan

<sup>5</sup>Research Institute for Electronic Science, Hokkaido University, Sapporo, 001-0021, Japan

[tokuda.kazuya.58z@st.kyoto-u.ac.jp](mailto:tokuda.kazuya.58z@st.kyoto-u.ac.jp)

**Key words:** picosecond phase change,  $\text{GeSbTe}$ , femtosecond laser, pump-probe, X-ray Free-Electron Laser.

## ABSTRACT

Dynamic picosecond lattice deformation of cubic  $\text{Ge}_2\text{Sb}_2\text{Te}_5$  phase-change alloy film (40 nm), induced by femtosecond near infrared (NIR) laser excitation (30 fs), was observed in picosecond scale for the first time. By means of ultrafast X-ray powder diffraction (XRPD) technique with repetitive NIR pump and X-ray Free Electron Laser (XFEL) probe, we have successfully observed the elapsed-time dependent of shifts of two Bragg diffractions. We have found the existence of large and anisotropic lattice deformation, which suggests a certain precursory behavior of picosecond phase changes recently reported. It is demonstrated that this technique has a high potential to unveil the mechanism of the picosecond phase changes and to develop future ultrafast phase-change devices.

## 1. INTRODUCTION

Femtosecond laser, possessing a pulse width less than the periods of atomic vibrations in solids, induces various intriguing phenomena including photo-induced phase-change phenomenon.<sup>[1]</sup> In the case of the Ge-Sb-Te (pseudobinary alloys of GeTe and  $\text{Sb}_2\text{Te}_3$ ) phase-change alloys,  $\text{Ge}_{10}\text{Sb}_2\text{Te}_{13}$  was reported to exhibit a drastic optical-reflectivity change that corresponds to the phase transition from crystal to amorphous in femtosecond scale.<sup>[2]</sup> Moreover, a possibility of picosecond-scale amorphization without going through the liquid phase was suggested by using a first-principle calculation and a kind of X-ray absorption spectroscopy.<sup>[3]</sup> These works suggest a feasibility of the development of future ultrafast phase-change devices. Such an ultrafast phase change process is expected to be different from the conventional one via the thermal process induced by commercially used nanosecond lasers, because the duration of femtosecond laser irradiation would be not enough for thermal diffusion while that of nanosecond laser is enough. While phase-change behaviors in nanosecond region are well-studied,<sup>[4]</sup> those induced by

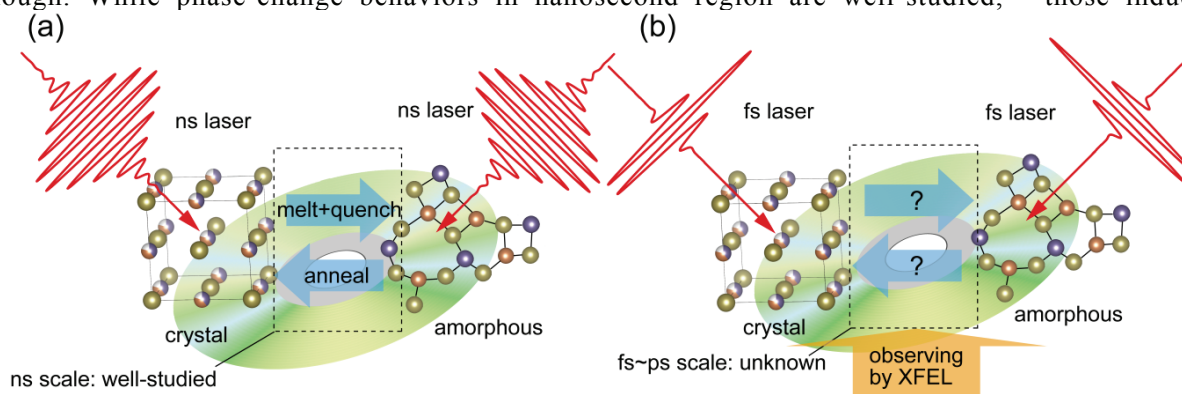


**Figure 1** Schematics of the phase changes between crystal and amorphous phase of  $\text{Ge}_2\text{Sb}_2\text{Te}_5$ , irradiated by (a) ns and (b) fs lasers.

<sup>a</sup>Present address : Department of Chemistry, School of Science, The University of Tokyo, Tokyo 113-0033, Japan

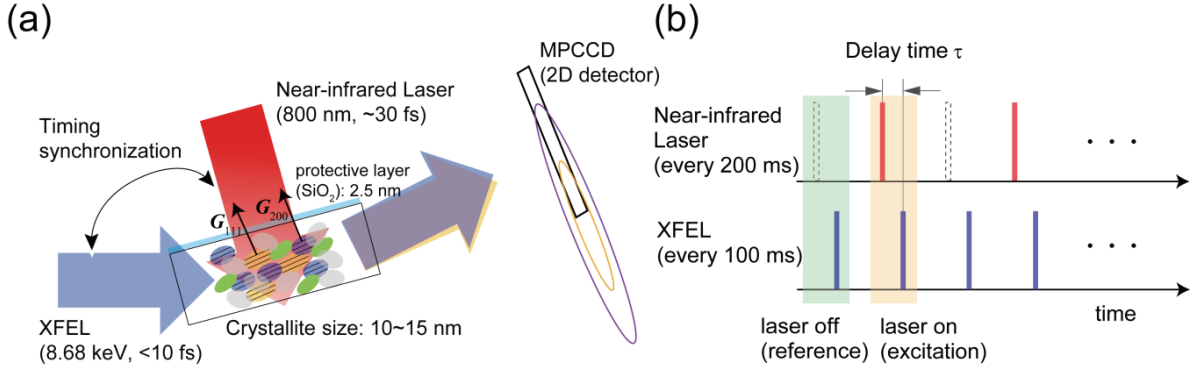


**Figure 2** (a) The optical geometry and (b) procedure of the NIR pump and X-ray probe measurements.

femtosecond laser have been still unknown due to the difficulty of the observation in such a short time scale. Although optical reflectivity measurements provide us much information with excellent time resolution in femtosecond or attosecond, they do not see one of the most essential information about the phase-change process, that is, the problem of how their atomic configuration changes.

Ultrafast X-ray diffraction (UXRD) with ultra-short pulse X-ray source is capable of answering this question. UXRD with conventional picosecond or femtosecond X-ray sources, e.g., a laser-plasma X-ray source and the pulse beam utilizing bunch structures of synchrotron radiation, have revealed ultrafast phenomena, e.g., lattice deformation,<sup>[5][6]</sup> coherent phonon oscillation,<sup>[7][8]</sup> non-thermal melting<sup>[9]</sup> and phase change.<sup>[1]</sup> However, these techniques were actually limited to highly crystalline samples such as single crystals or highly oriented crystals, because the brilliances of the conventional ultrafast X-ray sources were insufficient. In contrast, most of practical materials including GeSbTe are powder (polycrystalline) form. Therefore, a brilliant ultrafast X-ray source is required to measure UXRD for the powder samples. Recently, the development of femtosecond X-ray sources<sup>[10]</sup> have enabled us to measure for such kinds of samples. Especially, the advent of X-ray Free-Electron laser (XFEL),<sup>[11]</sup> which possesses ultra-short pulse width and significantly high brilliance, is expected to highly facilitate this measurement. Ultrafast X-ray powder diffraction (XRPD) using multi-dimensional detectors make it easy to observe multi peaks simultaneously. Moreover, we can observe even largely deformed lattice of powder samples, because both of original and deformed crystallites fulfill respective diffraction conditions in XRPD, while we cannot observe that of a single crystal because the large lattice change breaks diffraction condition ( $\mathbf{Q} = \mathbf{G}_{hkl}$ ). In this paper, we present our recent trials of XRPD with repetitive NIR pump and XFEL probe, conducted in Japanese XFEL facility SACLA,<sup>[12]</sup> for the typical phase-change material Ge<sub>2</sub>Sb<sub>2</sub>Te<sub>5</sub>.

## 2. EXPERIMENTS

Polycrystalline Ge<sub>2</sub>Sb<sub>2</sub>Te<sub>5</sub> thin films were prepared by RF magnetron sputtering and subsequent heat treatment. A Ge<sub>2</sub>Sb<sub>2</sub>Te<sub>5</sub> (40 nm) active layer and a SiO<sub>2</sub> (2.5 nm) cover layer were deposited on a Si (100) wafer, and heated at 235 °C under Ar atmosphere. The composition was Ge<sub>2</sub>Sb<sub>2</sub>Te<sub>4.86</sub>, determined by the ICP (inductively coupled plasma) analysis. The crystal structure was confirmed to be the same of reported metastable phase ( $Fm\bar{3}m$ ),<sup>[13]</sup> by conventional 2 $\theta$ - $\theta$  XRD measurement. The films were non-oriented and the estimated crystallite size was around 10-15 nm diameter. The thicknesses of layers were determined by the X-ray reflectivity measurement. Both the measurements were carried out by SmartLab diffractometer (Rigaku) using Cu K $\alpha$  parallel beam. The thickness of Ge<sub>2</sub>Sb<sub>2</sub>Te<sub>5</sub> film (40 nm) was set to NIR penetration depth ( $\sim 1/e^2$ ), which is sufficiently shorter than the penetration depth of X-ray.

The ultrafast XRPD measurements with NIR pump and XFEL probe were conducted at BL3 of SACLA.<sup>[14][15]</sup> Figure 2(a) shows its geometry (reflection configuration). The photon energy of incident X-ray was adjusted to 8.680 keV by tuning undulator and using Si (111) double crystal monochromater. The unfocused beam was guided to the sample with a beam size of 300  $\mu\text{m} \times 300 \mu\text{m}$ , restricted by quadrant slits. The samples were set at 15° from incident X-ray, where the footprint of the beam on the sample surface was 300  $\mu\text{m} \times 1160 (= 300 / \sin 15^\circ) \mu\text{m}$ . We used a Ti:sapphire NIR laser system with a wavelength of 800 nm and chirped amplifier for a pump light. The shape of NIR laser at the sample position was a circle of 800  $\mu\text{m}$  diameter with intensity distribution like Gaussian. The spatial overlap of NIR laser and XFEL was repeatedly checked by setting Ce:YAG fluorescent crystal. In this geometry, all delay times inevitably have an uncertainty of  $\pm 1.87$  ps, because the arrival timings at two ends of the XFEL's footprint on the sample are different. As shown in Figure 2(b), the SACLA XFEL was operated at 10 Hz repetition rate, and the NIR was operated at 5 Hz repetition rate. We took 500 shots for the reference state (without laser irradiation) and also for the excited state (with laser irradiation) in order to satisfy statistical quality of XRPD profiles. The pulse energy of

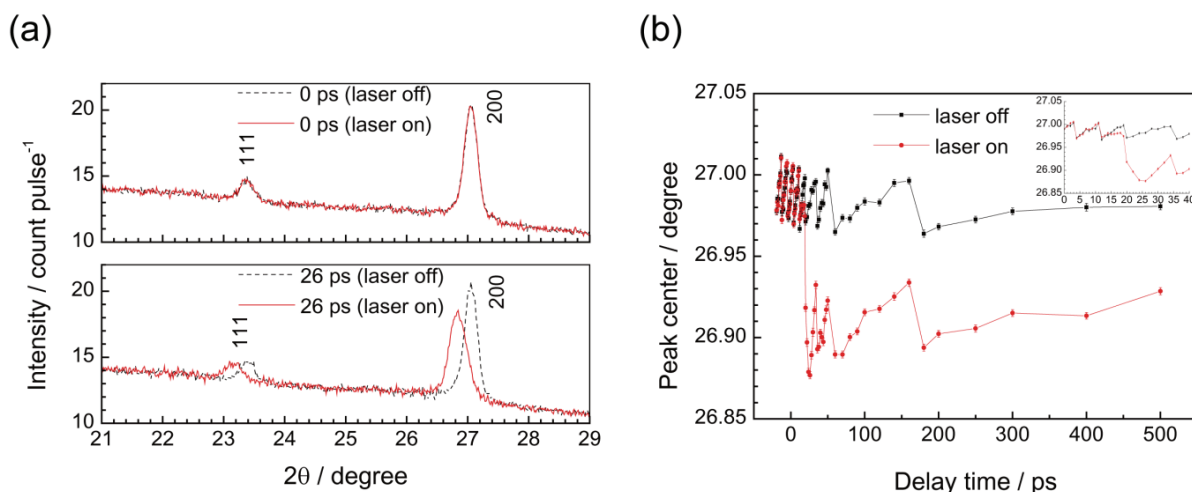


**Figure 3** (a) Typical XRPD profiles of laser off (reference) and on (excited), 500 shot averaged and 1D-converted. (b) Time evolution of peak center position of 200 reflection of laser off and on. Minus delay time means that XFEL arrives earlier than NIR laser. The inset is magnified at earlier stage.

NIR laser was set at 49 or 99  $\mu\text{J pulse}^{-1}$ , respectively. We checked that 500-shot accumulation of NIR laser with these fluences did not affect XRD profiles. Furthermore, the measurements at each time-delay were conducted at virgin places by parallel translations to circumvent the irradiation damages due to excessive accumulations. The origin of time delay at sample position was determined by monitoring direct X-ray and scattered NIR light from a thin sample at the sample position by the fast PIN diode connected to the 13 GHz oscilloscope. The accuracy of time-delay origin was estimated to be within  $\pm 10$  ps. The detector consists of  $1024 \times 512$  pixels (pixel size:  $50 \mu\text{m} \times 50 \mu\text{m}$ ) and the distance between the sample and detector surface was 259.8 mm; in this geometry, the scattering-angle range of about  $11.3^\circ$  around the fixed scattering angle  $2\theta_{\text{det}} = 25.4^\circ$ , was able to be detected simultaneously with an angular resolution of  $0.011^\circ$ . Some geometrical parameters of 2D detector (camera length, tilt angles or center pixel positions, etc) were determined by the diffraction of Ce:YAG polycrystal. By using these parameters, we converted obtained Debye rings into 1D profiles by following the reported procedures.<sup>[16]</sup> The fluctuation of XFEL intensity was normalized by the value of I0 monitor set downstream of monochromator.

### 3. RESULTS AND DISCUSSION

Figure 3 (a) shows the typical XRPD profiles for a laser-off state (reference state: upper) and for a laser-on state (excited state: lower). It is clearly seen that both 111 and 200 reflections shift to lower scattering angle suggesting the lattice expansion. To evaluate these shifts quantitatively, we conducted a profile-fitting with the split pseudo-Voigt function.<sup>[17]</sup> Figure 3 (b) is the elapsed-time dependence of peak-center angle of 200 reflections, error bars show standard deviations of least squares fitting calculated from variance-covariance matrix. The peak shift toward lower angle starts at around '14 ps'. (Note that the origin of this delay may have some extents of offset ( $\sim 20$  ps) as mentioned above and, therefore, we cannot discuss here the existence of incubation from this result.) The periodical fluctuations exist even in the profile of the laser-off state; this is a kind of experimental difficulty due to the imperfection of the parallelism between sample surface and translation plane. For comparison, we normalized the variations of lattice constants change in forms of expansion ratio through the Bragg's law. Figure 4(a) shows the time dependence of 200 reflections; the error bars were calculated from error-propagation equation. The extent of expansion is clearly proportional to the exciting laser fluence. Figure 4(b) compares the 111 and 200 reflections under the same excitation laser fluence (99  $\mu\text{J}$ ). Though small 111 reflection is not ideal in the statistical accuracy, it is very interesting that the expansion of the (111) inter-plane distance is significantly larger than the (200) inter-plane distance. The picosecond-expansion phenomenon itself is often seen in other materials,<sup>[5][6]</sup> but to our knowledge this laser-induced anisotropic expansion has not been reported to date. It is natural to regard that such a kind of deformation clearly differs from ordinary thermal expansion that retains cubic symmetry, and it would be a unique behavior of cubic  $\text{Ge}_2\text{Sb}_2\text{Te}_5$ . Further measurements by observing other directions (e.g. 220) and higher order reflections (e.g. 222) would be needed to comprehend this unique phenomenon deeply.

### 4. CONCLUSION

We applied ultrafast XRPD with repetitive NIR pump and XFEL probe measurement to  $\text{Ge}_2\text{Sb}_2\text{Te}_5$  metastable crystal phase. By observing two Bragg reflections simultaneously, we succeeded to find out the anomalous anisotropic

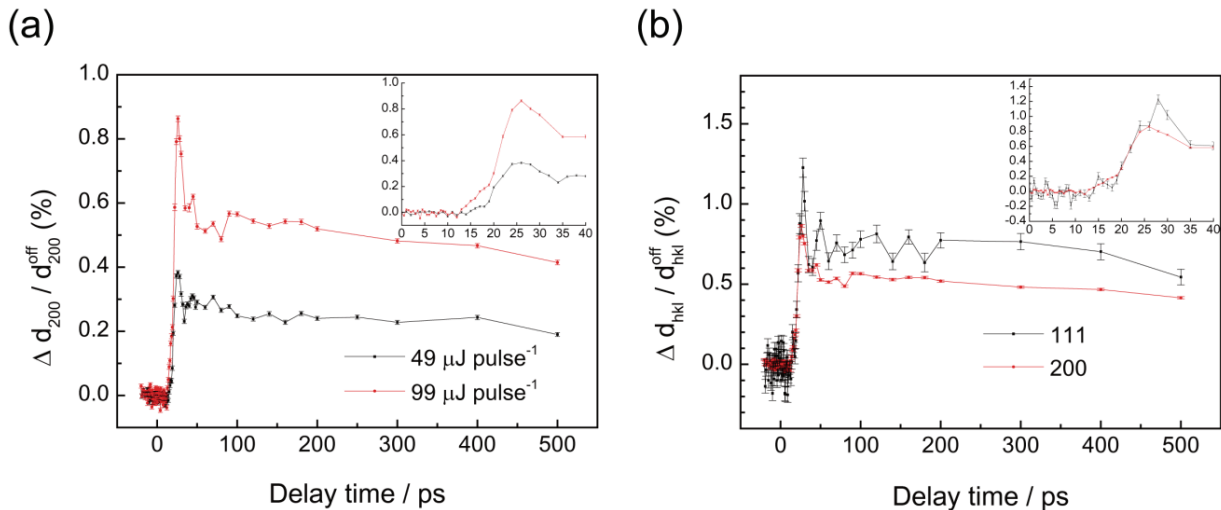


**Figure 4** (a) NIR laser fluence difference of time evolution of expansion calculated from 200 reflections. (b) Directional difference of time evolution of expansion at same NIR laser fluence ( $99 \mu\text{J pulse}^{-1}$ ).

expansion induced by the laser irradiation in the picosecond time scale. This anisotropic expansion is not an ordinary thermal expansion that should retain the cubic symmetry, and currently we are noticing as a certain kind of precursor phenomenon of the ultrafast phase change in this alloy. The present results suggest that this ultrafast XRPD technique can be effective for unveiling the precursory behavior in a phase-change process and this material would be used for future picosecond phase-change devices.

#### ACKNOWLEDGEMENTS

The crystal structures were illustrated by VESTA3<sup>[18]</sup>. We would like to thank Dr. M. Newton, Ms. R. Onitsuka, Mr. Y. Fujisawa and Ms. M. Sao for help the data acquisition and also the staff scientists at SACLA for keeping the high performance of the XFEL throughout our experiments. The experiments at SACLA were performed at the BL3 of SACLA with the approval of the Japan Synchrotron Radiation Research Institute (JASRI) (Proposal No.2012B8044). This work was supported by the X-ray Free Electron Laser Priority Strategy Program (MEXT).

#### REFERENCES

- [1] A. Cavalleri, C. Tóth, C. Siders, J. Squier, F. Ráksi, P. Forget, and J. Kieffer, *Phys. Rev. Lett.* **87**, 237401 (2001).
- [2] M. Konishi, H. Santo, Y. Hongo, K. Tajima, M. Hosoi, and T. Saiki, *Appl. Opt.* **49**, 3470 (2010).
- [3] A. Kolobov, P. Fons, M. Krbal, and J. Tominaga, *J. Non-Cryst. Solids* **358**, 2398 (2012).
- [4] Y. Fukuyama, N. Yasuda, J. Kim, H. Murayama, Y. Tanaka, S. Kimura, K. Kato, S. Kohara, Y. Moritomo, T. Matsunaga, R. Kojima, N. Yamada, H. Tanaka, T. Ohshima, and M. Takata, *Appl. Phys. Express* **1**, 045001 (2008).
- [5] P. Chen, I. Tomov, and P. Rentzepis, *J. Chem. Phys.* **104**, 10001 (1996).
- [6] C. Rose-Petruck *et al.*, *Nature* **398**, 310 (1999).
- [7] A. Lindenberg, I. Kang, S. Johnson, T. Missalla, P. Heimann, Z. Chang, J. Larsson, P. Bucksbaum, H. Kapteyn, H. Padmore, R. Lee, J. Wark, and R. Falcone, *Phys. Rev. Lett.* **84**, 111 (2000).
- [8] K. Sokolowski-Tinten, C. Blome, J. Blums, A. Cavalleri, C. Dietrich, A. Tarasevitch, I. Uschmann, E. Förster, M. Kammler, M. Horn-von-Hoegen, and D. von der Linde, *Nature* **422**, 287 (2003).
- [9] C. W. Siders, A. Cavalleri, K. Sokolowski-Tinten, C. Toth, T. Guo, M. Kammler, M. Horn von Hoegen, K. R. Wilson, D. von der Linde, and C. P. J. Barty, *Science*. **286**, 1340 (1999).
- [10] M. Hada and J. Matsuo, *X-Ray Spectrom.* **41**, 188 (2012).
- [11] P. Emma *et al.*, *Nat. Photon.* **4**, 641 (2010).
- [12] T. Ishikawa *et al.*, *Nat. Photon.* **6**, 540 (2012).
- [13] T. Matsunaga, N. Yamada, and Y. Kubota, *Acta Crystallogr., Sect. B Struct. Sci* **B60**, 685 (2004).
- [14] K. Tono, T. Togashi, and Y. Inubushi, *New J. Phys.* **15**, 083035 (2013).
- [15] T. Sato, T. Togashi, and K. Tono, *J. Phys. Conf. Ser.* **425**, 092009 (2013).
- [16] O. Shimomura, K. Takemura, H. Fujihisa, Y. Fujii, Y. Ohishi, T. Kikegawa, Y. Amemiya, and T. Matsushita, *Rev. Sci. Instrum.* **63**, 967 (1992).
- [17] H. Toraya, *J. Appl. Crystallogr.* **23**, 485 (1990).
- [18] K. Momma and F. Izumi, *J. Appl. Crystallogr.* **44**, 1272 (2011).